ACS APPLIED MATERIALS & INTERFACES

Article

Single Nanochannel-Aptamer-Based Biosensor for Ultrasensitive and Selective Cocaine Detection

Jian Wang, Jue Hou, Huacheng Zhang, Ye Tian, and Lei Jiang

ACS Appl. Mater. Interfaces, **Just Accepted Manuscript** • DOI: 10.1021/acsami.7b16539 • Publication Date (Web): 21 Dec 2017

ACS Publications

ACS Applied Materials & Interfaces is published by the American Chemical Society.
1155 Sixteenth Street N.W., Washington, DC 20036

Single Nanochannel-Aptamer-Based Biosensor for Ultrasensitive and Selective Cocaine Detection

Jian Wang,[†,‖] *Jue Hou,*[‡] *Huacheng Zhang,*[*,‡] *Ye Tian,*[⊥] *and Lei Jiang*[*,‖]

[†]College of Materials and Chemistry & Chemical Engineering, Chengdu University of Technology, Chengdu 610059, People's Republic of China

[‡]Department of Chemical Engineering, Monash University, Clayton, Victoria 3800, Australia

[⊥] Beijing National Laboratory for Molecular Sciences, Key Laboratory of Organic Solids, Institute of Chemistry, Chinese Academy of Sciences, Beijing 100190, People's Republic of China

[‖]Key Laboratory of Bio-inspired Materials and Interface Science, Technical Institute of Physics and Chemistry, Chinese Academy of Sciences, Beijing 100190, People's Republic of China

KEYWORDS: nanochannel sensor, DNA aptamers, cocaine detection, biosensor, drug testing

ABSTRACT: Ultrasensitive and selective detection of molecules at nano or sub-nanomolar level is very important for many areas such as early diagnosis and drug testing. Herein, we report a high-sensitive cocaine sensor based on a single nanochannel coupled with DNA aptamers. The single nanochannel-aptamer-based biosensor can recognize cocaine molecules with an excellent sensitivity and good selectivity. A linear relationship between target cocaine concentration and output ionic current is obtained in a wide concentration range of cocaine from 1 nM to 10 μM. The cocaine sensor also shows a detection limit down to 1 nM. This study provides a new avenue

to develop new nanochannel-aptamer-based biosensors for rapid and ultratrace detection of a variety of illicit drugs.

INTRODUCTION

Synthetic nanochannels[1-9] have attracted great attention in the past decade because they can exhibit similar or stronger functionality, superior stability and robustness compared to fragile biological channels. The nanochannel-based biosensors[10-14] have been proved to have many advantages than other sensors, such as simplicity, high sensitivity, rapid and reversible response, label-free, and high signal-to-noise ratios.[15-16] Single nanochannel-based platforms have been widely used as resistive-pulse sensors for sensing charged polymers,[17-18] proteins,[13, 19-20] and DNAs.[21-22] In the resistive-pulse sensing technique, the charged molecules and electrolyte ions were driven by an applied external voltage to pass through the nanochannels. Obvious occlusions of transmembrane ionic currents of the nanochannels were observed when the charged molecules entered the nanochannels, while the transmembrane ionic currents could recover again when the charged molecules exited the nanochannels. For example, single porphyrin molecule (~2 nm in diameter) has been detected by a cone-shaped polyimide nanochannel with a tip opening of ~4.5 nm. The diameter of the single porphyrin molecule is comparable to the channel diameter, when the porphyrin molecules transported through the conical nanochannel, a number of ionic current occlusion events could be detected.[23] However, if molecular size of the analyte (i.e. small molecules and metal ions) is much smaller than the diameter of nanochannel, the occlusion events cannot be observed by the resistive-pulse technique.[24]

To achieve detection of small analytes using nanochannels, steady-state analysis approaches[2] have been recently developed. Functional molecules, such as amino acids, crown ethers and

proteins, have been used to modify the inner surfaces of the nanochannels to be the specific recognition sites of the small analytes. The functionalized nanochannels could exhibit different ion transport properties before and after binding of target analytes because the analyte binding onto the recognition sites of the nanochannel could lead to obvious changes of the surface charge, effective diameter and/or wettability of the channel, thus achieving detection of small molecules,[25-27] metal ions,[28-31] and metal ion-molecular complexes.[32-33] Compared with other functional molecules, DNA aptamers have been recently recognized as a more effective tool in construction of biosensors for small molecular sensing.[20, 34-38] Aptamers with specific binding features have been successfully used to fabricate electrochemical,[39-40] fluorescence,[41-42] and colorimetric[43-44] biosensors for various drug detections. Electrochemical biosensors have been recognized as a convenient and robust platform for target detection, but need tedious electrode modification and subsequent operations, which are time-consuming and also affect the reproducibility.[45] Fluorescent techniques possess a high sensitivity and excellent selectivity for the detection of many target analytes, but still have limits like high background noise, false positive signals, and difficulty in labeling probes.[15] Colorimetric aptamer-sensors have attracted much attention due to their practicality, portability, and improved reproducibility, however, the preparation of nanoparticles, complicated samples pretreatment, and low sensitivity still limit their applications.[15, 40] Therefore, it remains challenging to develop simple, convenient, and effective platforms for highly sensitive drug detections. Single nanochannels combined with DNA aptamers are supposed to be efficient platforms to achieve ultrasensitive drug detections.

In this work, we report an artificial single nanochannel-aptamer-based biosensor for ultrasensitive and selective recognition of cocaine. The sensor is constructed by immobilization of capture DNA aptamers (C-aptamers) onto the inner wall of single nanochannels. The C-

aptamers can selectively bind cocaine and target DNA aptamer molecules (T-aptamers) onto the channel wall, resulting partial or complete occlusion of the channel and shield of the channel surface charge, thus to reduce the transmembrane ionic current of the nanochannel. As a result, cocaine detection in the nanochannel-aptamer-based biosensor can be easily achieved by measuring ionic current changes of the channel before and after binding of cocaine and T-aptamer molecules. The nanochannel-aptamer-based sensor exhibits an ultrahigh sensitivity of cocaine down to 1 nM level and a remarkable specificity toward cocaine over other small drugs of similar structures. This work, as an example, provides a basic strategy for further developing diverse nanochannel-aptamer-based molecular biosensors with an ultrahigh sensitivity, inherent simplicity, and real-time monitoring property for efficient drug detections and clinical diagnostics in the future.

EXPERIMENTAL SECTION

Materials. Phosphate buffered saline (PBS), tropinone ($C_8H_{13}NO$, 99%), atropine ($C_{17}H_{23}NO_3$, ≥ 99%), and glucose (D-glucose, ≥ 99.5%) were purchased from Sigma-Aldrich (China). N-hydroxysulfosuccinimide sodium salt (NHSS, 97%) and 1-(3-dimethylaminopropyl)-3-ethylcarbodiimide hydrochloride (EDC, 98+%) were purchased from Alfa Aesar (China). Potassium chloride (KCl, 99.8%), potassium hydroxide (KOH, 98.0%), sulfuric acid (H_2SO_4, 95.0%-98.0%), and sodium hydroxide (NaOH, 96.0%) were purchased from Sinopharm Chemical Reagent Beijing (China). Formic acid (HCOOH, ≥ 88%), and hydrochloric acid (HCl, 36.0%-38.0%) were purchased from Beijing Chemical Works (China). Cocaine hydrochloride was purchased from Beijing Institute for Drug Control (Beijing, China), and then dissolved in PBS buffer solution (0.01 M, pH 7.4) to different concentrations (from 1 nM to 500 μM). DNA

oligonucleotides were synthesized by Takara Biotechnology Co. Ltd. (Dalian, China). Unless otherwise stated, the chemical solutions were prepared using MilliQ water (18.2 MΩ).

Nanochannel Fabrication. Polyethylene terephthalate (PET) membranes (Hostaphan RN12 Hoechst, 12 μm thick) with single heavy ion track in the center were chemically etched to fabricate single bullet-shaped nanochannels within the membranes using a asymmetric track-etching technique.[46] During the etching process, the PET film was immobilized between two chambers of a custom-designed etching cell. One side of the film was etched by 6 M NaOH solution, while the other side was etched by 6 M NaOH + 0.025 wt% surfactant solution at 60 °C. The surfactant used here is sodium dodecyl diphenyloxide disulfonate. To monitor the etching process, transmembrane ionic current of the PET film was measured at a constant voltage of 1.0 V. After the current reached the desired value, etching solutions of both sides of the PET membrane were replaced by a stopping solution (including 1 M KCl + 1 M HCOOH) to neutralize the etchant and stop the etching process. To remove residual salts inside the single bullet-shaped nanochannel, the etched PET nanochannel membrane was washed by water for 3 times and soaked in MilliQ water overnight.

Capture DNA Immobilization. C-aptamers were successively grafted onto the inner wall of the nanochannel by a two-step chemical modification method. Prior to the modification, carboxyl groups created on the nanochannel wall were activated in 4 mL PBS (0.01 M, pH 7.4) solution containing 30 mg/mL EDC and 6 mg/mL NHSS for 2 h. Then, the nanochannel membrane was treated by 1 μM capture DNA (0.01 M PBS, pH 7.4) solution for 12 h to graft C-aptamers onto the channel wall. Finally, the modified nanochannel membrane was washed by water for 3 times and stored in MilliQ water before further experiments.

Preparation of the Mixed Solution Containing Target DNA and Cocaine. 1 mM stock cocaine solution was prepared from Cocaine hydrochloride with PBS buffer (pH 7.4) at room temperature. T-aptamers were also dissolved in PBS buffer solution. Cocaine solutions were then diluted to different concentrations (including 1 nM, 10 nM, 100 nM, 1 μM, 10 μM, 100 μM, and 500 μM). The mixed solutions of 1 μM T-aptamer and different concentrations of cocaine were also prepared in the PBS buffer. The cocaine solutions and the mixed solutions containing cocaine and T-aptamer were used to be electrolytes in the current measurement.

Current-Voltage (*I-V*) Measurement and Real-Time Current Recordings. Ionic transport properties of the nanochannels before and after modification were evaluated by the *I-V* curves and ionic current recordings with a Keithley 6487 picoammeter (Keithley Instruments, Cleveland, OH) in different electrolyte solutions (0.1 M KCl, 1 M KCl, and 0.01 M PBS, respectively). A pair of Ag/AgCl electrodes were applied to the two sides of the nanochannel membrane to apply a transmembrane potential across the nanochannel. The cathode faced the large opening (base) side of the channel, while the anode faced the small opening (tip) side. Scanning voltages varied from -2 V to + 2 V with a 21 s period were used for *I-V* measurement and a constant voltage of +2 V was used for real-time current recording. All measurements were carried out at room temperature, and each test was repeated five times to obtain the average value.

Characterization. A FEI Magellan 400 extreme high resolution scanning electron microscope (SEM) was used to characterize the nanochannel samples at an acceleration voltage of 5 kV. X-ray photoelectron spectroscopy (XPS) analysis of PET membrane before and after modification was performed by the Thermo Scientific ESCALab 250Xi using 200 W monochromated Al Kα radiation, 500 μm X-ray spot, and ~3×10^{-10} mbar of base pressure in the chamber. The hydrocarbon C1s lines at 284.8 eV from adventitious carbon is used for energy referencing. The

analysis software was used as provided by the instrument's manufacturer. Because no other new element was introduced after every step of modification, the peak of nitrogen (N1s) was used to reflect the modification process. Contact angles (CAs) were measured using an OCA 20 instrument (DataPhysics, Germany) at room temperature and saturated humidity. MilliQ water (18.2 MΩ) was used for the CA measurement. In each measurement, a 2-μL droplet of water was dispensed onto the substrates for investigation. The PET films for CA measurements was prepared under the same condition as the single nanochannel membrane.

RESULTS AND DISCUSSION

The design strategy of the nanochannel-aptamer-based cocaine sensor is shown in Scheme 1. A single bullet-shaped nanochannel with a length of 12 μm was prepared by asymmetrically etching single-ion-tracked PET membrane, as described in our previous work.[46] Here we fabricate bullet-shaped single nanochannels to be the platform to develop cocaine sensor, because it has been less used to develop nanodevices, compared with other cylinder-, cone-, and hourglass-shaped nanochannels.[47] Furthermore, the bullet-shaped nanochannel has been proved to have a good stability and reproducibility,[48] as well as a more pronounced rectifying behavior than the conical nanochannel.[49-51] A SEM image of the cross section of a single nanochannel confirmed its bullet-like shape (Figure S1a in the Supporting Information (SI)). SEM images of the two sides of the nanochannel membrane also well illustrated that the nanochannel has a large opening (base side) and a small opening (tip side), respectively, at its two ends (Figures S1b and S1c in SI). The base diameter is 174.3 ± 23.5 nm, while the tip diameter is 30.2 ± 5.1 nm (Figures S1d and S1e in SI). As the inner surface of the PET nanochannel possessed carboxyl groups that were produced during the etching process,[52-55] C-aptamer (molecular size of ~5.4 nm in diameter) was grafted onto the channel wall by a two-step modification method.[46, 56] C-

aptamers immobilized on the nanochannel wall are single-stranded and then fold into double-stranded structures after binding of cocaine and T-aptamer molecules.[57] After capturing of cocaine and T-aptamer, the effective diameter of the nanochannel for ionic transport was reduced because of the bodipy493/503-modified T-aptamer with a molecular size of ~9.1 nm.[20] Therefore, the cocaine detection can be achieved by measuring the ionic current changes of the C-DNA-modified nanochannel before and after binding of cocaine and T-aptamer molecules.

In order to confirm the successful binding of cocaine and T-aptamer molecules on the nanochannel wall, CA and XPS measurements were employed to characterize the surface of the PET membrane before and after modification. CAs of the PET membrane at original, etched, C-DNA-modified and cocaine/T-aptamer-bound states are 84.4 ± 0.7°, 72.8 ± 1.1°, 55.1 ± 1.3° and 60.1 ± 1.9°, respectively (Figure 1a). The CA values were obtained from the averages of five drops at different locations of the membrane. Insets are the corresponding photographs of water droplet shapes on the PET film. All these changes of wettability on the PET membrane corresponded to the change of chemical composition. Figure 1b shows XPS spectra of the membrane before and after immobilization of C-aptamer, and after binding of cocaine and T-aptamer (see Tables S1, S2, and S3 in the SI for more information). Different from the unmodified membrane, typical N1s XPS peaks at near 400 eV were observed for the membrane after C-aptamer modification and binding of cocaine and T-aptamer, indicating that aptamers were successfully immobilized onto the membrane surface. To further confirm the assembly of cocaine and T-aptamer molecules on the PET membrane, fluorescence tests were also conducted on the membrane surface. The fluorescence intensity was investigated by exciting the PET membrane at 488 nm and measuring the emission at 510 nm. The T-aptamer has a fluorescent group on its 5' end with excitation peak at 493 nm, and emission peak at 503 nm. After binding

of T-aptamer, an obvious emission peak at ~510 nm was observed (Figure 1c). These results provide an important evidence for the successful binding of cocaine and T-aptamer molecules onto the surface of the C-aptamer-modified PET membrane.

For the single bullet-shaped nanochannel, its DNA modification was confirmed by measuring the transmembrane ionic current of the channel before and after modification in 0.1 M and 1 M potassium chloride and 0.01 M PBS (pH 7.4) solutions. As shown in Figure S2 in SI, *I-V* characteristic and rectification ratio changes of the single nanochannel before and after C-aptamer modification were observed remarkably, which could be mainly ascribed to the blockage effect of the C-aptamer molecules. Real-time current recording of the nanochannel was monitored at +2 V in PBS solution, and the difference in the electronic signature of current traces of the channel before and after modification was apparent (Figure S3 in SI). These results indirectly confirmed the successful immobilization of C-aptamer molecules onto the channel wall, and the C-aptamer-modified single nanochannel could function as a nanofluidic platform for cocaine sensing.

The sensing performance of the nanochannel-aptamer-based platform was systematically investigated by measuring the *I-V* properties of the C-aptamer-modified nanochannel under PBS solutions with and without cocaine and/or T-aptamer molecules. Figure 2a depicts *I-V* curves of the C-DNA-modified nanochannel measured in 0.01 M PBS with and without addition of 1 μM cocaine and/or 1 μM T-aptamer molecules. *I-V* characteristics suggest no sensing happened in the modified nanochannel without T-Aptamer, while the ionic current and rectification ratio of the nanochannel significantly decreased after simultaneous addition of cocaine and T-aptamers (Figure S4 in SI). This clearly confirmed the successful anchoring of cocaine and T-aptamer onto the inner wall of the nanochannel, and the experimental results also imply that the presence of T-

DNA aptamers is essential for cocaine detection in the nanochannel-aptamer-based sensor. Current change ratios, $(I_0-I)/I_0$, defined here as the absolute value of the current variation, recorded at a +2 V bias with 1 μM target cocaine with or without T-aptamer, are presented in Figure 2b. It is evident that the modified nanochannel with T-aptamer displayed good selectivity to cocaine, and the presence of target cocaine could be well monitored via the ionic current change of the nanochannel.

The sensitivity of the nanochannel-aptamer-based sensor was evaluated by testing the current properties of the C-aptamer-modified nanochannel under different cocaine concentrations, together with 1 μM target aptamers in 0.01 M PBS buffer (pH 7.4). The ionic current decreased accordingly with increase of the cocaine concentration, and the currents measured under 0 M, 1 nM, and 1 μM cocaine conditions were 7.03 ± 0.04, 6.56 ± 0.04, and 5.69 ± 0.05 nA, respectively (Figure S5 in SI). The binding of cocaine and T-aptamer molecules onto the nanochannel wall led to a significant decrease in the effective size, thereby affecting the ion flux across the nanochannel membrane (Figure 3a). The anchoring of cocaine and T-aptamer molecules could also shield the negative surface charge of the nanochannel, in agreement with the decrease observed in the nanochannel rectification ratio, from 4.26 ± 0.01 (0 M) to 2.96 ± 0.13 (1 μM). As shown in Figure 3a, the cocaine recognition process coupled with the formation of ligand-receptor conjugates that were supramolecularly confined within the nanochannel. The effective diameter of the nanochannel gradually reduced with increasing the binding amount of cocaine molecules and T-aptamers: (I) the nanochannel without cocaine and T-aptamer complexes showed high ionic current, (II) the effective diameter of the nanochannel reduced partly and showed relative low ionic current as the C-aptamer sites were partly bound with cocaine and T-aptamer complexes under low cocaine concentration, and (III) the effective

diameter of the nanochannel decreased furtherly and displayed extreme low ionic current when the C-aptamer sites were fully bound with cocaine and T-aptamer complexes under high cocaine concentration. With increasing the binding of target cocaine and T-aptamer complexes (II, III), such large supramolecular complexes could gradually block the nanochannel and shield the negative surface charge of the nanochannel, leading to different levels of pore occlusion.[32]

Figure 3b displays the current ratio changes of the nanochannel-aptamer-based sensor measured at +2 V under different cocaine concentrations (0 M, 1 nM, 10 nM, 100 nM, 1 μM, 10 μM, 100 μM, and 500 μM, respectively) in the absence or presence of 1 μM T-aptamer. The ionic current of the sensor decreased gradually with increasing cocaine concentration of the PBS solutions with 1 μM T-aptamer from 1 nM to 500 μM, whereas the current was almost constant (ratio $\approx$ 1) without T-aptamer in the same concentration range. The corresponding *I-V* curves of the nanochannel were shown in Figure S6 in SI. A linear relationship between target cocaine concentration and output ionic current was observed in a wide concentration range from 1 nM to 10 μM of cocaine, exhibiting a detection limit down to 1 nM (Figure 3b). The experimental results confirmed that the nanochannel-aptamer-based sensor has excellent sensitivity of cocaine at ultratrace concentrations. Such a high cocaine sensitivity of the nanochannel-aptamer-based sensor at nanomolar level is better than those of other reported traditional aptamer-based cocaine sensor (see Table S4 in SI), showing potential practical applications in clinical diagnostics and drug testing.

To further verify the selectivity of the nanochannel-aptamer-based cocaine sensor, binding effects of the sensor of cocaine over other small molecules with similar chemical structures as cocaine, including glucose, atropine, and tropinone were investigated. *I-V* characteristics of a reproduced C-aptamer-modified nanochannel were systematically measured in 0.01 M PBS

solutions with 1 μM of each target molecule and 1 μM T-aptamer (see Figure S7 in SI). The ionic current measured at +2 V for each analyte became different, and a significant change for target cocaine was observed. Current change ratios, $(I_0-I)/I_0$, defined here as the absolute value of the current variation, recorded at +2 V bias with cocaine and other nonspecific small molecules of similar structures, are presented in Figure 4. A relatively high current-change ratio of ~0.29 can be obtained in the presence of cocaine, while the ratios calculated from other nonspecific molecules were ~0.22, ~0.19, and ~0.14, respectively. From the variations in the current-change ratio of the nanochannel-aptamer-based cocaine sensor, we can conclude that the sensor presented displays a remarkable specificity toward cocaine. Due to the inherent selectivity of aptamers for the target molecule, the artificial single-nanochannel-based platform has potential application in recognition of cocaine.

CONCLUSION

In conclusion, a single nanochannel-aptamer-based biosensor for highly sensitive and selective cocaine recognition has been fabricated by integrating single artificial nanochannels with DNA aptamers. The biosensor showed a good selectivity and excellent sensitivity toward cocaine over other drugs with similar chemical structures. A linear relationship between target cocaine concentration and output ionic current was observed in a wide concentration range from 1 nM to 10 μM of cocaine, showing a detection limit down to 1 nM level. This new nanochannel-aptamer-based biosensor shows better cocaine sensitivity and selectivity over traditional sole aptamer-based cocaine sensors, which confirms that the integration of single nanochannels with functional aptamers is expected to be an effective way to design new biosensing devices for ultrasensitive and selective drug detections in the fields of medicine, healthcare, food, and environment.

ASSOCIATED CONTENT

Supporting Information. SEM images of the cross section, the base and the tip side of the bullet-shaped nanochannel membrane, XPS data, *I-V* curves and real-time current recording of the nanochannel before and after C-aptamer modification, *I-V* properties of the nanochannel-aptamer-based sensor measured under different conditions, and a systematic comparison of the cocaine detection performance between sole aptamer-based methods and our nanochannel-aptamer-based sensor. This material is available free of charge via the Internet at http://pubs.acs.org.

AUTHOR INFORMATION

Corresponding Author

*E-mail: huacheng.zhang@monash.edu

*E-mail: jianglei@iccas.ac.cn

Author Contributions

The manuscript was written through contributions of all authors. All authors have given approval to the final version of the manuscript.

Notes

The authors declare no competing financial interest.

ACKNOWLEDGMENT

This research is financially supported by the National Research Fund of China for Fundamental Key Projects (2013CB932802), the National Natural Science Foundation of China (21501185

and 21671194), the Australian Research Council (DE170100006), and the Key Research Program of the Chinese Academy of Sciences (KJZD-EW-M03), the 111 project (B14009).

REFERENCES

(1) Daiguji, H. Ion Transport in Nanofluidic Channels. *Chem. Soc. Rev.* **2010**, *39*, 901-911.

(2) Zhang, H.; Tian, Y.; Jiang, L. Fundamental Studies and Practical Applications of Bio-Inspired Smart Solid-State Nanopores and Nanochannels. *Nano Today* **2016**, *11*, 61-81.

(3) Kowalczyk, S. W.; Blosser, T. R.; Dekker, C. Biomimetic Nanopores: Learning from and About Nature. *Trend. Biotechnol.* **2011**, *29*, 607-614.

(4) Ali, M.; Ahmed, I.; Nasir, S.; Ramirez, P.; Niemeyer, C. M.; Mafe, S.; Ensinger, W. Ionic Transport through Chemically Functionalized Hydrogen Peroxide-Sensitive Asymmetric Nanopores. *ACS Appl. Mater. Interfaces* **2015**, *7*, 19541-19545.

(5) Hou, X.; Guo, W.; Jiang, L. Biomimetic Smart Nanopores and Nanochannels. *Chem. Soc. Rev.* **2011**, *40*, 2385-2401.

(6) Hou, X.; Zhang, H.; Jiang, L. Building Bio-Inspired Artificial Functional Nanochannels: From Symmetric to Asymmetric Modification. *Angew. Chem. Int. Ed.* **2012**, *51*, 5296-5307.

(7) Zhang, H.; Hou, X.; Hou, J.; Zeng, L.; Tian, Y.; Li, L.; Jiang, L. Synthetic Asymmetric-Shaped Nanodevices with Symmetric pH-Gating Characteristics. *Adv. Funct. Mater.* **2015**, *25*, 1102-1110.

(8) Zhang, H.; Tian, Y.; Hou, J.; Hou, X.; Hou, G.; Ou, R.; Wang, H.; Jiang, L. Bioinspired Smart Gate-Location-Controllable Single Nanochannels: Experiment and Theoretical Simulation. *ACS Nano* **2015**, *9*, 12264-12273.

(9) Kong, Y.; Fan, X.; Zhang, M.; Hou, X.; Liu, Z.; Zhai, J.; Jiang, L. Nanofluidic Diode Based on Branched Alumina Nanochannels with Tunable Ionic Rectification. *ACS Appl. Mater. Interfaces* **2013**, *5*, 7931-7936.

(10) Howorka, S.; Siwy, Z. Nanopore Analytics: Sensing of Single Molecules. *Chem. Soc. Rev.* **2009**, *38*, 2360-2384.

(11) de la Escosura-Muñiz, A.; Merkoçi, A. Nanochannels Preparation and Application in Biosensing. *ACS Nano* **2012**, *6*, 7556-7583.

(12) Jiang, Y.; Guo, W. Nanopore-Based Sensing and Analysis: Beyond the Resistive-Pulse Method. *Sci. Bull.* **2015**, *60*, 491-502.

(13) Takakura, T.; Yanagi, I.; Goto, Y.; Ishige, Y.; Kohara, Y. Single-Molecule Detection of Proteins with Antigen-Antibody Interaction Using Resistive-Pulse Sensing of Submicron Latex Particles. *Appl. Phys. Lett.* **2016**, *108*, 123701.

(14) Shi, W.; Friedman, A. K.; Baker, L. A. Nanopore Sensing. *Anal. Chem.* **2017**, *89*, 157-188.

(15) Rauf, S.; Zhang, L.; Ali, A.; Liu, Y.; Li, J. Label-Free Nanopore Biosensor for Rapid and Highly Sensitive Cocaine Detection in Complex Biological Fluids. *ACS Sens.* **2017**, *2*, 227-234.

(16) Hou, X.; Jiang, L. Learning from Nature: Building Bio-Inspired Smart Nanochannels. *ACS Nano* **2009**, *3*, 3339-3342.

(17) Robertson, J. W. F.; Rodrigues, C. G.; Stanford, V. M.; Rubinson, K. A.; Krasilnikov, O. V.; Kasianowicz, J. J. Single-Molecule Mass Spectrometry in Solution Using a Solitary Nanopore. *Proc. Natl. Acad. Sci. U. S. A.* **2007**, *104*, 8207-8211.

(18) Reiner, J. E.; Kasianowicz, J. J.; Nablo, B. J.; Robertson, J. W. F. Theory for Polymer Analysis Using Nanopore-Based Single-Molecule Mass Spectrometry. *Proc. Natl. Acad. Sci. U. S. A.* **2010**, *107*, 12080-12085.

(19) Harrington, L.; Alexander, L. T.; Knapp, S.; Bayley, H. Pim Kinase Inhibitors Evaluated with a Single-Molecule Engineered Nanopore Sensor. *Angew. Chem. Int. Ed.* **2015**, *54*, 8154-8159.

(20) Li, T.; Liu, L.; Li, Y.; Xie, J.; Wu, H. C. A Universal Strategy for Aptamer-Based Nanopore Sensing through Host–Guest Interactions inside A-Hemolysin. *Angew. Chem. Int. Ed.* **2015**, *54*, 7568-7571.

(21) Keyser, U. F.; Koeleman, B. N.; van Dorp, S.; Krapf, D.; Smeets, R. M. M.; Lemay, S. G.; Dekker, N. H.; Dekker, C. Direct Force Measurements on DNA in a Solid-State Nanopore. *Nat. Phys.* **2006**, *2*, 473-477.

(22) Haque, F.; Li, J.; Wu, H. C.; Liang, X. J.; Guo, P. Solid-State and Biological Nanopore for Real-Time Sensing of Single Chemical and Sequencing of DNA. *Nano Today* **2013**, *8*, 56-74.

(23) Heins, E. A.; Siwy, Z. S.; Baker, L. A.; Martin, C. R. Detecting Single Porphyrin Molecules in a Conically Shaped Synthetic Nanopore. *Nano Lett.* **2005**, *5*, 1824-1829.

(24) Kawano, R.; Osaki, T.; Sasaki, H.; Takinoue, M.; Yoshizawa, S.; Takeuchi, S. Rapid Detection of a Cocaine-Binding Aptamer Using Biological Nanopores on a Chip. *J. Am. Chem. Soc.* **2011**, *133*, 8474-8477.

(25) Han, C.; Hou, X.; Zhang, H.; Guo, W.; Li, H.; Jiang, L. Enantioselective Recognition in Biomimetic Single Artificial Nanochannels. *J. Am. Chem. Soc.* **2011**, *133*, 7644-7647.

(26) Sun, Z.; Han, C.; Song, M.; Wen, L.; Tian, D.; Li, H.; Jiang, L. Fabrication of Cysteine-Responsive Biomimetic Single Nanochannels by a Thiol-Yne Reaction Strategy and Their Application for Sensing in Urine Samples. *Adv. Mater.* **2013**, *26*, 455-460.

(27) Hou, G.; Zhang, H.; Xie, G.; Xiao, K.; Wen, L.; Li, S.; Tian, Y.; Jiang, L. Ultratrace Detection of Glucose with Enzyme-Functionalized Single Nanochannels. *J. Mater. Chem. A* **2014**, *2*, 19131-19135.

(28) Hou, X.; Yang, F.; Li, L.; Song, Y.; Jiang, L.; Zhu, D. A Biomimetic Asymmetric Responsive Single Nanochannel. *J. Am. Chem. Soc.* **2010**, *132*, 11736-11742.

(29) Tian, Y.; Hou, X.; Wen, L.; Guo, W.; Song, Y.; Sun, H.; Wang, Y.; Jiang, L.; Zhu, D. A Biomimetic Zinc Activated Ion Channel. *Chem. Commun.* **2010**, *46*, 1682-1684.

(30) Ali, M.; Nasir, S.; Ramirez, P.; Cervera, J.; Mafe, S.; Ensinger, W. Calcium Binding and Ionic Conduction in Single Conical Nanopores with Polyacid Chains: Model and Experiments. *ACS Nano* **2012**, *6*, 9247-9257.

(31) Perez-Mitta, G.; Albesa, A. G.; Knoll, W.; Trautmann, C.; Toimil-Molares, M. E.; Azzaroni, O. Host-Guest Supramolecular Chemistry in Solid-State Nanopores: Potassium-Driven Modulation of Ionic Transport in Nanofluidic Diodes. *Nanoscale* **2015**, *7*, 15594-15598.

(32) Ali, M.; Nasir, S.; Nguyen, Q. H.; Sahoo, J. K.; Tahir, M. N.; Tremel, W.; Ensinger, W. Metal Ion Affinity-Based Biomolecular Recognition and Conjugation inside Synthetic Polymer Nanopores Modified with Iron–Terpyridine Complexes. *J. Am. Chem. Soc.* **2011**, *133*, 17307-17314.

(33) Boussouar, I.; Chen, Q.; Chen, X.; Zhang, Y.; Zhang, F.; Tian, D.; White, H. S.; Li, H. Single Nanochannel Platform for Detecting Chiral Drugs. *Anal. Chem.* **2017**, *89*, 1110-1116.

(34) Ali, M.; Nasir, S.; Ensinger, W. Bioconjugation-Induced Ionic Current Rectification in Aptamer-Modified Single Cylindrical Nanopores. *Chem. Commun.* **2015**, *51*, 3454-3457.

(35) Guo, W.; Hong, F.; Liu, N.; Huang, J.; Wang, B.; Duan, R.; Lou, X.; Xia, F. Target-Specific 3d DNA Gatekeepers for Biomimetic Nanopores. *Adv. Mater.* **2015**, *27*, 2090-2095.

(36) Burns, J. R.; Seifert, A.; Fertig, N.; Howorka, S. A Biomimetic DNA-Based Channel for the Ligand-Controlled Transport of Charged Molecular Cargo across a Biological Membrane. *Nat. Nanotech.* **2016**, *11*, 152-156.

(37) Chao, J.; Zhu, D.; Zhang, Y.; Wang, L.; Fan, C. DNA Nanotechnology-Enabled Biosensors. *Biosens. Bioelectron.* **2016**, *76*, 68-79.

(38) Tan, Z.; Feagin, T. A.; Heemstra, J. M. Temporal Control of Aptamer Biosensors Using Covalent Self-Caging to Shift Equilibrium. *J. Am. Chem. Soc.* **2016**, *138*, 6328-6331.

(39) Golub, E.; Pelossof, G.; Freeman, R.; Zhang, H.; Willner, I. Electrochemical, Photoelectrochemical, and Surface Plasmon Resonance Detection of Cocaine Using Supramolecular Aptamer Complexes and Metallic or Semiconductor Nanoparticles. *Anal. Chem.* **2009**, *81*, 9291-9298.

(40) Bozokalfa, G.; Akbulut, H.; Demir, B.; Guler, E.; Gumus, Z. P.; Odaci Demirkol, D.; Aldemir, E.; Yamada, S.; Endo, T.; Coskunol, H.; Timur, S.; Yagci, Y. Polypeptide Functional Surface for the Aptamer Immobilization: Electrochemical Cocaine Biosensing. *Anal. Chem.* **2016**, *88*, 4161-4167.

(41) He, J. L.; Wu, Z.-S.; Zhou, H.; Wang, H. Q.; Jiang, J.-H.; Shen, G. L.; Yu, R. Q. Fluorescence Aptameric Sensor for Strand Displacement Amplification Detection of Cocaine. *Anal. Chem.* **2010**, *82*, 1358-1364.

(42) Hou, J.; Zhang, H.; Yang, Q.; Li, M.; Song, Y.; Jiang, L. Bio-Inspired Photonic-Crystal Microchip for Fluorescent Ultratrace Detection. *Angew. Chem. Int. Ed.* **2014**, *53*, 5791-5795.

(43) Du, Y.; Li, B.; Guo, S.; Zhou, Z.; Zhou, M.; Wang, E.; Dong, S. G-Quadruplex-Based Dnazyme for Colorimetric Detection of Cocaine: Using Magnetic Nanoparticles as the Separation and Amplification Element. *Analyst* **2011**, *136*, 493-497.

(44) Soh, J. H.; Lin, Y.; Rana, S.; Ying, J. Y.; Stevens, M. M. Colorimetric Detection of Small Molecules in Complex Matrixes Via Target-Mediated Growth of Aptamer-Functionalized Gold Nanoparticles. *Anal. Chem.* **2015**, *87*, 7644-7652.

(45) Tan, Y.; Wei, X.; Zhao, M.; Qiu, B.; Guo, L.; Lin, Z.; Yang, H. H. Ultraselective Homogeneous Electrochemical Biosensor for DNA Species Related to Oral Cancer Based on Nicking Endonuclease Assisted Target Recycling Amplification. *Anal. Chem.* **2015**, *87*, 9204-9208.

(46) Wang, J.; Fang, R.; Hou, J.; Zhang, H.; Tian, Y.; Wang, H.; Jiang, L. Oscillatory Reaction Induced Periodic C-Quadruplex DNA Gating of Artificial Ion Channels. *ACS Nano* **2017**, *11*, 3022-3029.

(47) Hou, X.; Liu, Y.; Dong, H.; Yang, F.; Li, L.; Jiang, L. A pH-Gating Ionic Transport Nanodevice: Asymmetric Chemical Modification of Single Nanochannels. *Adv. Mater.* **2010**, *22*, 2440-2443.

(48) Pavel Yu, A.; Irina, V. B.; Sergei, N. D.; Oleg, L. O.; Adam, P.; Bozena, A. S. Fabrication of Nanopores in Polymer Foils with Surfactant-Controlled Longitudinal Profiles. *Nanotechnology* **2007**, *18*, 305302.

(49) Patricio, R.; Pavel Yu, A.; Javier, C.; Salvador, M. Pore Structure and Function of Synthetic Nanopores with Fixed Charges: Tip Shape and Rectification Properties. *Nanotechnology* **2008**, *19*, 315707.

(50) Pavel Yu, A.; Irina, V. B.; Oleg, L. O.; Patricio, R.; Bozena, A. S. Effect of Nanopore Geometry on Ion Current Rectification. *Nanotechnology* **2011**, *22*, 175302.

(51) Perez-Mitta, G.; Tuninetti, J. S.; Knoll, W.; Trautmann, C.; Toimil-Molares, M. E.; Azzaroni, O. Polydopamine Meets Solid-State Nanopores: A Bio-Inspired Integrative Surface

Chemistry Approach to Tailor the Functional Properties of Nanofluidic Diodes. *J. Am. Chem. Soc.* **2015**, *137*, 6011-6017.

(52) Siwy, Z.; Apel, P.; Dobrev, D.; Neumann, R.; Spohr, R.; Trautmann, C.; Voss, K. Ion Transport through Asymmetric Nanopores Prepared by Ion Track Etching. *Nucl. Instrum. Methods Phys. Res., Sect. B* **2003**, *208*, 143-148.

(53) Zhang, H.; Hou, X.; Yang, Z.; Yan, D.; Li, L.; Tian, Y.; Wang, H.; Jiang, L. Bio-Inspired Smart Single Asymmetric Hourglass Nanochannels for Continuous Shape and Ion Transport Control. *Small* **2015**, *11*, 786-791.

(54) Harrell, C. C.; Siwy, Z. S.; Martin, C. R. Conical Nanopore Membranes: Controlling the Nanopore Shape. *Small* **2006**, *2*, 194-198.

(55) Zhang, H.; Hou, J.; Ou, R.; Hu, Y.; Wang, H.; Jiang, L. Periodic Oscillation of Ion Conduction of Nanofluidic Diodes Using a Chemical Oscillator. *Nanoscale* **2017**, *9*, 7297-7304.

(56) Liu, Q.; Wen, L.; Xiao, K.; Lu, H.; Zhang, Z.; Xie, G.; Kong, X. Y.; Bo, Z.; Jiang, L. A Biomimetic Voltage-Gated Chloride Nanochannel. *Adv. Mater.* **2016**, *28*, 3181-3186.

(57) Cho, E. J.; Lee, J. W.; Ellington, A. D. Applications of Aptamers as Sensors. *Annu. Rev. Anal. Chem.* **2009**, *2*, 241-264.

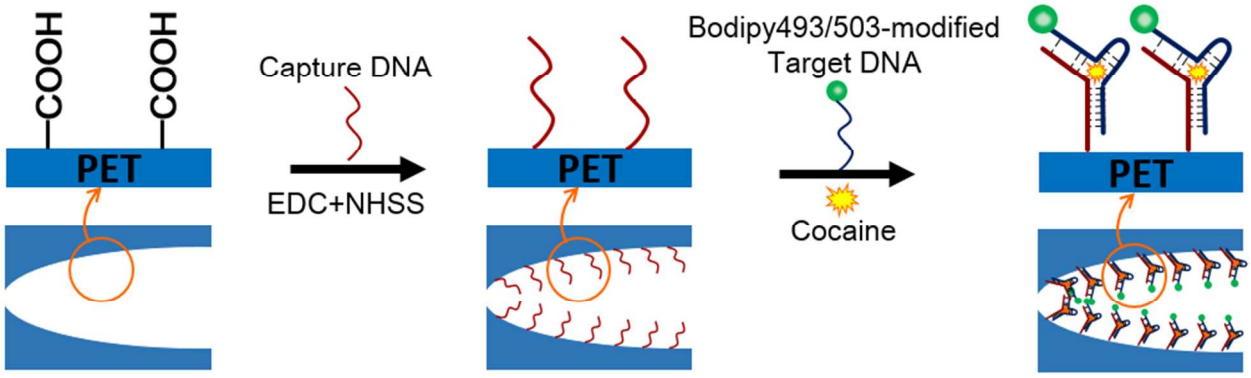

Scheme 1. Schematic representation of a high-sensitive aptamer-based cocaine detector using an engineered single nanochannel. Single-stranded capture DNA were firstly used to functionalize the single bullet-shaped nanochannel, and then folded into double-stranded structure by cocaine binding, altering electron transfer and reducing the ionic current, and cocaine could be directly detected by the transmembrane current recording. The oligonucleotide sequence (5' to 3') of Capture DNA is 5'-NH_2-$(CH_2)_3$GGGAGTCAAGAACGAA-3', and the oligonucleotide sequence (5' to 3') of Target DNA is 5'-Bodipy493/503-TTCGTTCTTCAATGAAGTGGGACGACA-3'. The scheme is not drawn to scale.

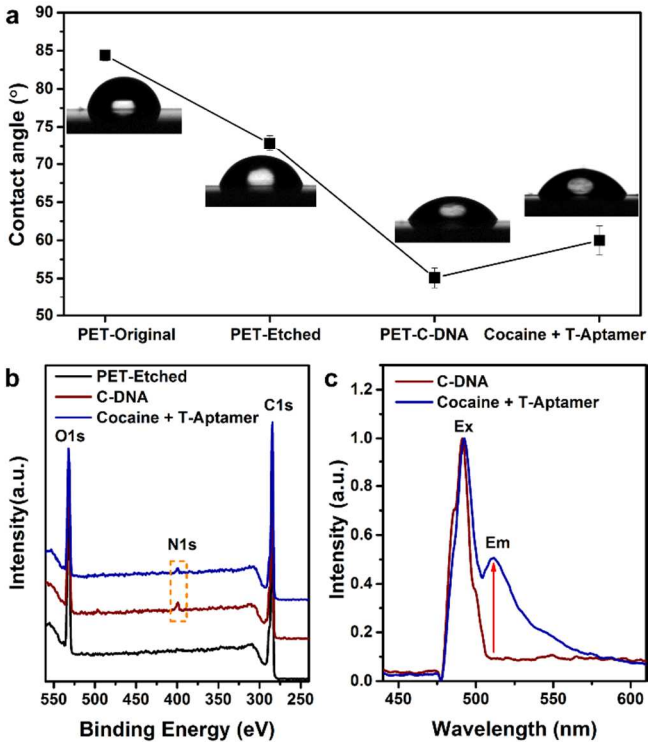

Figure 1. Contact angle, XPS, and fluorescence spectra results of the PET membrane. (a) Contact angles of the PET film at each consequential experimental procedures are 84.4 ± 0.7°, 72.8 ± 1.1°, 55.1 ± 1.3°, and 60.1 ± 1.9°, respectively. Insets are the corresponding photographs

of water droplet shape on the PET film. The data were obtained from five independent measurements and the error bars indicate the standard deviation. (b) XPS spectra of the PET film before and after capture DNA aptamers modification and after target DNA aptamers addition. (c) Fluorescence spectra of the PET surface after capture-DNA aptamer modification in the absence/presence of target-DNA aptamer (T-Aptamer). The fluorescence intensity was monitored by exciting the PET membrane at 488 nm and measuring the emission at 510 nm. The target aptamer has a fluorescent group on its 5' end with excitation peak (Ex) at 493 nm, and emission peak at 503 nm. After T-Aptamer addition, an obvious emission peak (Em) at ~510 nm was observed, in contrast with the sample without T-Aptamer.

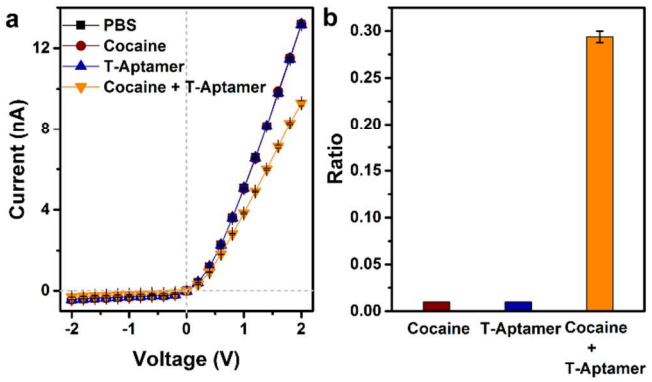

Figure 2. The discriminating property of 1 μM target cocaine in the single-nanochannel-based platform without or with addition of 1 μM target aptamers, as labeled. (a) *I-V* curves measured in 0.01 M PBS (pH = 7.4) with or without T-Aptamer at a scanning voltage varied from -2 to +2 V with a 21 s period. (b) Comparison of the current change ratios, $(I_0\text{-}I)/I_0$, recorded at +2 V with 1 μM target cocaine in the proposed platform with or without T-Aptamer, where I_0 and I are the current measured in the absence and presence of target analytes. The data represent the averages and standard deviations from five independent experiments.

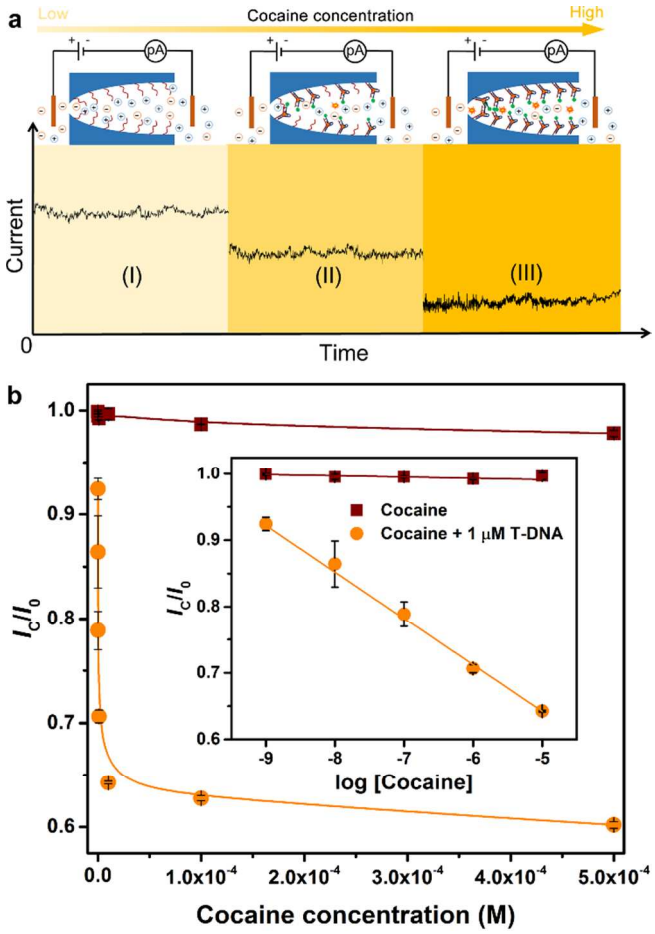

Figure 3. Cocaine recognition with a DNA-aptamer-modified single bullet-shaped nanochannel-based platform. (a) Schematic representation of the cocaine detection mechanism with (I) non-cocaine-bound C-Aptamer, and (II, III) cocaine-bound states of C-aptamers (form aptamer complexes). Cocaine could be directly detected by monitoring of ionic current signals, and the current decreases as the cocaine concentration increases. (b) Comparison of the current ratios, I_c/I_0, recorded at +2 V with different concentration of target cocaine in the proposed platform with or without T-Aptamer, where I_c is the ionic current measured at different cocaine concentrations and I_0 is the current measured in the absence of cocaine. The data represent the averages and standard deviations from five independent experiments.

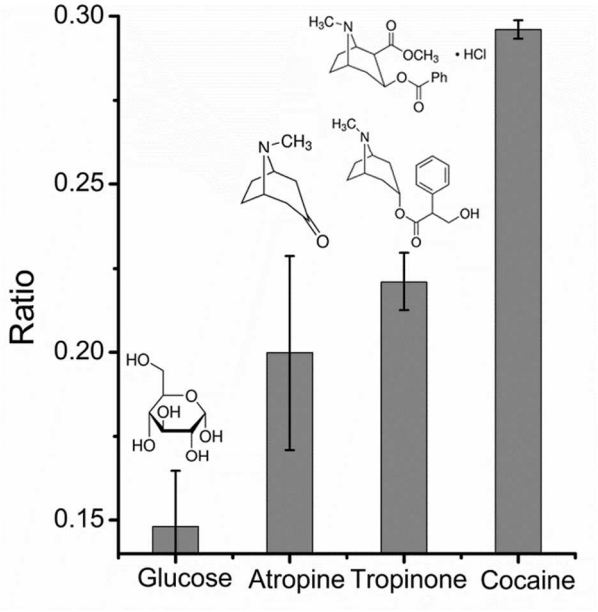

Figure 4. Selectivity of the DNA-aptamer-modified single nanochannel-based platform. Comparison of the current change ratios, $(I_0\text{-}I)/I_0$, recorded at +2 V with target cocaine and other nonspecific small molecules, where I_0 and I are the current measured in the absence and presence of target analytes. Experiments were performed in four different solutions with the concentration of 1 μM for glucose, atropine, tropinone, and cocaine, respectively, containing 0.01 M PBS buffer (pH 7.4), and 1 μM T-Aptamer. Insets are the structural formulae of each molecules. The data represent the averages and standard deviations from five independent experiments.

Table of Contents Graphic